A Generalizable Framework for Print Defect Detection using Frequency Filtering and Data-Driven Feature Selection

WonWoo No
Manufacturing AI Research Center
Korea Institute of Industrial Technology
Incheon, Korea
nhowonwoo98@kitech.re.kr

Hyunchul Tae
Manufacturing AI Research Center
Korea Institute of Industrial Technology
Incheon, Korea
sage@kitech.re.kr

Abstract

This paper proposes a novel machine learning-based system for detecting micro-defects in high-quality prints by leveraging a rich set of pattern matching features. To ensure robustness against variations between the digital truth (DT) and the captured vision truth (VT) images, we first apply a **frequency-domain correction** to suppress noise and amplify defect signals. From the corrected images, we initially construct a comprehensive, 42-dimensional hybrid feature vector for each image patch, which includes statistical, **LBP-based textural**, and **SIFT-based structural features**. A feature importance analysis is then conducted, and a final compact feature set comprising only the top 10 most influential features is selected for training a Light GBM model. This approach allows the system to distinguish true defects from natural print texture variations with high accuracy and efficiency. Experimental results are expected to show that this pattern-enhanced approach significantly outperforms methods based on simple difference metrics, especially in reducing false positives on complex backgrounds.

Keywords: *Defect Detection, Pattern Recognition, Light GBM, LBP, SIFT, Quality Control.*

I. INTRODUCTION

Automated Optical Inspection (AOI) is a critical component in modern manufacturing for ensuring product quality [5]. In the high-quality printing industry, a key challenge is the reliable detection of micro-defects from captured images (VT/VF) by comparing them against a digital master (DT). However, conventional methods that rely on simple image subtraction are notoriously sensitive to environmental variations such as inconsistent illumination and color tone shifts, often leading to an unacceptably high rate of false positives [1].

To overcome this, our research focuses on a machine learning approach engineered for robustness. While texture descriptors like LBP [3] and structural key point detectors like SIFT [4] have been used effectively in isolation, their true potential lies in a synergistic combination. Our primary contribution is a novel framework that integrates a specialized preprocessing step with a data-driven feature selection process. We first employ **a frequency-domain correction designed to be robust against lighting and color variations**, which actively suppresses noise while amplifying true defect signals. We then construct a comprehensive **pattern-enhanced feature vector** that combines statistical, textural, and structural information. Crucially, we demonstrate that a compact subset of these features—specifically, the top 10 most influential features identified through model analysis—is sufficient for high-performance classification. This results in an efficient and highly accurate Light GBM-based system capable of discerning subtle defects from complex background patterns..

II. METHOD

1) Preprocessing

Defects manifest as high-frequency signals, while global illumination shifts are low-frequency phenomena [2]. To robustly isolate defects, we perform a frequency-domain correction. First, the DT and VT images are transformed into the frequency domain using a 2D Fourier Transform($\mathcal{F}$).

$$\mathrm{F_{DT}}(u,v) = \mathcal{F}\{\mathrm{DT}(x,y)\},$$
$$\mathrm{F_{VT}}(u,v) = \mathcal{F}\{\mathrm{VT}(x,y)\}$$

We then define a low-pass filter $\mathrm{H}_{LP}(u,v)$ (e.g., a Gaussian filter) and a corresponding high-pass filter $\mathrm{H}_{HP}(u,v) = 1 - \mathrm{H}_{LP}(u,v)$. A composite frequency representation, $\mathrm{H}_{corr}(u,v)$, is created by combining the low-frequency components from the DT with the high-frequency components from the VT, actively suppressing low-frequency noise and amplifying high-frequency defect signals:

$$\mathrm{F_{corr}}(u,v) = F_{DT}(u,v) * H_{LP}(u,v) + F_{VT}(u,v) * H_{HP}(u,v)$$

Finally, an inverse Fourier transform ($\mathcal{F}^{-1}$) yields the corrected VT image, $\mathrm{VT_{corr}}(x,y)$, which is globally aligned with the DT, with background noise minimized and critical defect information enhanced.

$$\mathrm{VT_{corr}}(x,y) = \mathcal{F}^{-1}\{F_{corr}(u,v)\}$$

2) Feature Engineering and Selection

The core of our system is a two-step process of comprehensive feature extraction followed by data-driven feature selection to build a discriminative and efficient model.

2.2.1. Pattern-Enhanced Feature Vector Construction

A rich, 42-dimensional feature vector, V_{patch}, is extracted from each corresponding patch pair (P_{DT}, P_{corr}) of the DT and the corrected VT. This vector is a concatenation of four distinct feature groups:

$$V_{patch} = [v_{stat} || v_{LBP} || v_{sift} || v_{sim}]$$

Where, || denotes concatenation.

- Statistical & Difference Features (v_{stat}): This group quantifies the basic intensity and error signals. It includes the mean, standard deviation, median, max, and min values for both P_{DT} and P_{corr} as well as statistics from their absolute difference image.

-Texture Analysis using LBP (v_{LBP}): To capture fine textural variations, we utilize Local Binary Patterns [3]. For each patch, a histogram of uniform LBP patterns is computed. The feature vector v_{LBP} includes statistics of the LBP image (mean, std, variance) and

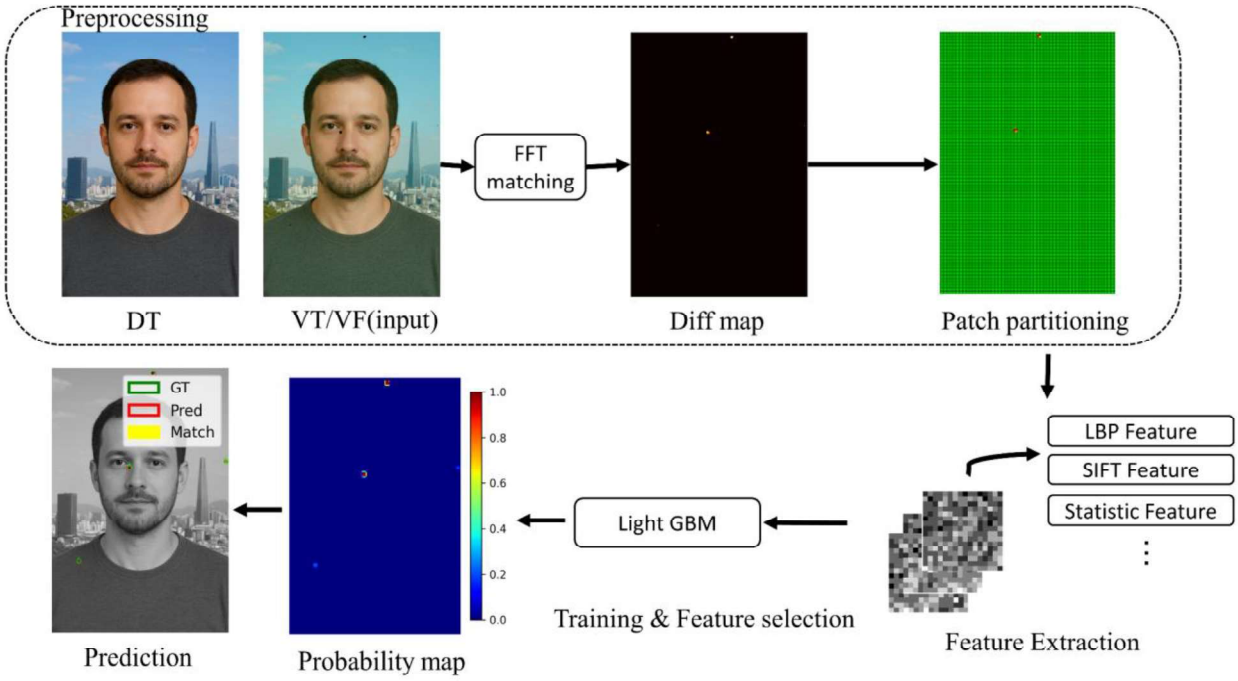

Figure 1. Flow Chart

the top bins of the histogram, effectively describing the patch's micro-pattern composition.

-Structural Analysis using SIFT (v_{sift}): To measure structural changes, we apply the SIFT detector [4] on each patch. Instead of using the descriptors directly, we extract statistics from the detected key points, forming a feature vector v_{sift} that includes: the total number of key points (N_{kp}), the spatial variance of key point locations (σ^2_{pos}) and statistics of key point scales and orientations. This provides a robust signature of the patch's structural complexity.

-Similarity Analysis (v_{sim}): A direct measure of similarity is calculated using Normalized Cross-Correlation (NCC) between the two patches, providing a global similarity score.

2.2.2. Feature Selection

While the 42-D vector is comprehensive, not all features contribute equally. To create a more efficient and robust model, a feature selection process is performed. An initial Light GBM model is trained using all 42 features to rank them based on their feature importance (gain). **The top 10 most influential features are then selected to form the final** (V_{sel}), compact feature vector used for training the definitive model. This step eliminates redundant information and focuses the model on the most discriminative patterns.

3) Classification and Postprocessing

The final stage of the system translates the extracted feature vectors into a clean, interpretable defect map. The selected 10-dimensional feature vectors (V_{sel}) are first normalized using a StandardScaler, where each feature x_i in the vector is transformed to its scaled version x_i':

$$x_i' = \frac{x_i - \mu_i}{\sigma_i}$$

Here, μ_i and σ_i are the mean and standard deviation of the ith feature, respectively. These scaled feature vectors are then input into a trained Light GBM model, which outputs a probability score p ∈ [0,1] for each patch. These scores are assembled into a raw probability map $P(x,y)$. This raw map is first converted into a binary mask $M_b(x,y)$ by applying an optimized threshold τ :

$$M_b(x,y) = \begin{cases} 1 & \text{if } P(x,y) > \tau \\ 0 & otherwise \end{cases}$$

To regularize the mask, a sequence of morphological operations is applied using a structuring element K. A morphological opening ($M_b \circ K$) removes small noise, and a subsequent closing ($M_b \cdot K$) fills minor gaps. The final refinement step involves analyzing each remaining connected component (contour) C. A component is retained only if it satisfies a set of geometric constraints:

$$\text{Area}(C) \in [A_{min}, A_{max}] \wedge AspectRatio(C) \in [R_{min}, R_{max}]$$

This filtering ensures that only objects with defect-like morphology are present in the defect mask.

III. Experiments and Result.

1) Experimental setup

The system's generalization capability was evaluated on a private industrial dataset of 19 distinct print groups, collected from a commercial photo card manufacturing process. Due to a non-disclosure agreement, this dataset cannot be made publicly available. These were partitioned into a training set (11 groups), validation set (3 groups), and test set (5 groups). To demonstrate the importance of diverse data, we compare two models:

-Model_SG (single- Group): Trained and validated using data from only one group (group_1)

-Model_MG (Multi-Group): Trained and validated using data from all 14 training/validation groups.

Performance was measured using object-based metrics (Precision, Recall, F1-Score). Model_SG was evaluated on a held-out portion of its own group_1 data (seen domain), while Model_MG was evaluated on the unseen test set of 150 images from 5 groups (unseen domain)

2) Quauntative Results

The experimental results, summarized in Table 1, highlight the trade-off between specialization and generalization. Model_SG achieves an impressive F1-score of 0.8895 on its own familiar data, establishing a benchmark for in-domain, overfitted performance. However, a model overfitted to one domain is not practical for industrial use.

Our proposed Model_MG, trained on diverse data, demonstrates strong generalization. It achieves a high mean F1-score of 0.8603 across all 5 unseen test groups. A particularly noteworthy finding, detailed in Table 3, is the performance on group_11. On this unseen group, Model_MG reached an F1-score of 0.949, This demonstrates that the multi-group training strategy not only provides robust average performance but can also achieve better accuracy on entirely new data.

Group	Mean Score (per image)		
	Precision	***Recall***	***F-1 Score***
Single-Group	0.9040	0.9475	0.8895
Multi-Group	0.8528	0.9359	0.8603

Table 1. Overall Performance Summary (Averaged per Images)

The consistency of Model_MG across different unseen groups is also high, with a low standard deviation of 0.068 between the group-average F1-scores, indicating reliable performance regardless of the print batch.

# of Group	Mean Score (per image)		
	Precision	***Recall***	***F-1 Score***
13	0.819	0.990	0.849
8	0.826	0.939	0.843
11	0.956	0.973	0.949
17	0.917	0.920	0.910
7	0.746	0.857	0.751

Table 2. Inter-Group Performance Consistency of Model_MG

3) Qualitive Analysis

The qualitative results mirrored the quantitative findings. Model_MG proved highly robust, correctly identifying 664 out of 696 total defects across the test set (95.4% recall). While its aggregated object precision was 47.0%, indicating some over-sensitivity, this was mainly concentrated in a few highly challenging images (e.g., group_8/img-0330.png, F1-score: 0.000). The model's ability to achieve perfect scores (F1-score: 1.000) on many other images (e.g., group_13/img-0041.png) underscores its effectiveness.

IV. CONCLUSION AND FUTURE WORK

This paper quantitatively demonstrated the necessity of a multi-group training strategy for building a truly generalizable defect detection system. While a model specialized to a single domain (Model_SG) can achieve high in-domain accuracy, it fails to adapt to new data. Our proposed model (Model_MG), trained on a diverse dataset, not only achieves robust average performance on unseen data but also shows it can reach near-specialized performance (F1-score of 0.949) on certain new domains. This proves that diverse training is not just a defensive measure against performance degradation but a proactive strategy to achieve high, consistent accuracy in real-world industrial applications. Future work could explore adaptive thresholding techniques to further reduce false positives.

REFERENCE

[1] C. I. Tsai, D. M. Tsai, "A difference image-based defect detection algorithm for digital print quality inspection," Journal of Imaging Science and Technology, 2008.

[2] Y. F. Chen, M. C. Lu, "Automatic Defect Detection in Printed Circuit Boards Using A Frequency Domain Approach," IEEE Transactions on Instrumentation and Measurement, 2008.

[3] M. A. Suhail, T. S. Obaid, "Fabric Defect Detection Using Local Binary Patterns and Support Vector Machines," Journal of Engineering and Technology, 2013.

[4] D. G. Lowe, "Distinctive image features from scale-invariant keypoints," International journal of computer vision, 2004.

[5] D. M. Tsai, "A survey on automated surface inspection using machine vision," Proc. of the Int. Conf. on Mechatronics and Automation, 2013